Stirring in the global surface ocean

Darryn W. Waugh[1] and Edward R. Abraham[2]

Received 30 July 2008; revised 26 August 2008; accepted 15 September 2008; published 24 October 2008.

[1] Global variations of stirring in the surface ocean are quantified using finite-time Lyapunov exponents (FTLEs) calculated from currents derived from satellite altimetry. It is shown that the stirring is highly non-uniform, and the probability distribution functions (PDFs) of the FTLEs are broad, asymmetric, and have long high-stretch tails. The characteristics of the PDFs vary with mesoscale activity and integration time: There are larger values and broader PDFs in regions of high strain rates and eddy kinetic energy (EKE), e.g., western boundary currents and the Antarctic Circumpolar Current, and for shorter integration times. The PDFs have a near-universal relationship with the mean strain of a region, and are reasonably well fit by Weibull distributions. The above variations in the stirring may help our understanding of the distribution and spatial heterogeneities of biogeochemical tracers, and raise the possibility of developing a parameterization of the stirring based on the, easily-calculated, EKE. **Citation:** Waugh, D. W., and E. R. Abraham (2008), Stirring in the global surface ocean, *Geophys. Res. Lett.*, *35*, L20605, doi:10.1029/2008GL035526.

1. Introduction

[2] Quantifying horizontal dispersal and mixing in the ocean surface is important for understanding a wide range of problems, including understanding the spatial distribution of temperature and chlorophyll [*Abraham and Bowen*, 2002; *Mahadevan and Campbell*, 2002], plankton dynamics [*Martin*, 2003], and larval transport [e.g., *Chiswell et al.*, 2003]. In recent years several studies have quantified aspects of the horizontal dispersion in the ocean surface [e.g., *Abraham and Bowen*, 2000; *d'Ovidio et al.*, 2004; *Lacorata et al.*, 2001; *LaCasce and Ohlmann*, 2003; *Marshall et al.*, 2006; *Beron-Vera et al.*, 2008; *Rossi et al.*, 2008]. However, these studies have generally focused on limited ocean regions and used different data sets and diagnostics. As a result these studies cannot be easily combined to examine global variations in the horizontal dispersion.

[3] Here we examine global variations in the stirring by calculating finite-time Lyapunov exponents (FTLEs) using a single data source: surface geostrophic currents derived from satellite-altimeter measurements. *Waugh et al.* [2006] (hereinafter referred to as W06) performed similar calculations in the Tasman Sea and showed that in this region there is large variability in the FTLEs, and that the regional scale variability is related to variations in mesoscale activity. However, it is not known if these results are universal, and we examine here how the distributions of FTLEs vary over the globe.

2. Data and Methods

[4] The surface ocean currents used in this study are derived from satellite altimeter measurements of sea level. Gridded absolute geostrophic velocities were obtained from the Archiving Validation and Interpretation of Satellite Data in Oceanography. These geostrophic velocities are calculated from absolute sea level height that is the sum of merged altimeter measurements of anomalous sea level and the mean dynamic topography of *Rio and Hernandez* [2004]. The gridded data are on a 1/3 degree Mercator grid and are available every 7 days.

[5] The stirring is quantified by calculating FTLEs, where the FTLE at location $\mathbf{x}_0$ and time t_0 is

$$\lambda(\mathbf{x}(\mathbf{x}_0, t_0), \tau) = \frac{1}{\tau} \log\left(\frac{|\delta\mathbf{x}(\tau)|}{|\delta\mathbf{x}(0)|}\right), \quad (1)$$

where $\delta\mathbf{x}(\tau)$ is the separation at time $t_0 + \tau$ between two points which were close together and centered at location $\mathbf{x}_0$ at time t_0, and the orientation of $\delta\mathbf{x}(0)$ is chosen so that λ is maximal. In a pure-strain flow an initially small, circular patch of tracer will be deformed into an ellipse, and the FTLE equals the rate of increase of the major axis of this ellipse, which is equal to the strain rate. For time-varying flows with spatially varying deformation fields the FTLE is no longer simply the local instantaneous strain rate, but is related to the integrated strain encountered along a parcel trajectory. FTLEs can be used to understand and quantify the dispersal of tracer patches [e.g., *Abraham et al.*, 2000; W06] and to interpret structure in observed tracer fields [e.g., *Pierrehumbert and Yang*, 1993; *Neufeld et al.*, 2000; *Abraham and Bowen*, 2002].

[6] We calculate FTLEs in the same manner as by *Abraham and Bowen* [2002], where full details are given. Briefly, λ is calculated from the logarithm of the largest eigenvalue of $\mathbf{M}^\mathbf{T}\mathbf{M}$, where $\mathbf{M}$ is the deformation obtained by integrating the Jacobian of the flow along a trajectory. Trajectories are calculated using fourth-order Runge-Kutta integration with a daily time-step. Linear interpolation from the gridded velocities and finite differencing is used to calculate the Jacobian at any point. The full velocity field is used for the trajectories, but only the traceless component of the Jacobian is used to obtain $\mathbf{M}$, which ensures that the λ are always positive.

[7] FTLEs are calculated for trajectories initialized on a regular 0.5° longitude by 0.5° latitude grid. Because the geostrophic balance used to determine the surface currents does not hold at the equator we do not perform calculations

[1]Department of Earth and Planetary Science, Johns Hopkins University, Baltimore, Maryland, USA.
[2]Dragonfly, Island Bay, Wellington, New Zealand.

0094-8276/08/2008GL035526$05.00

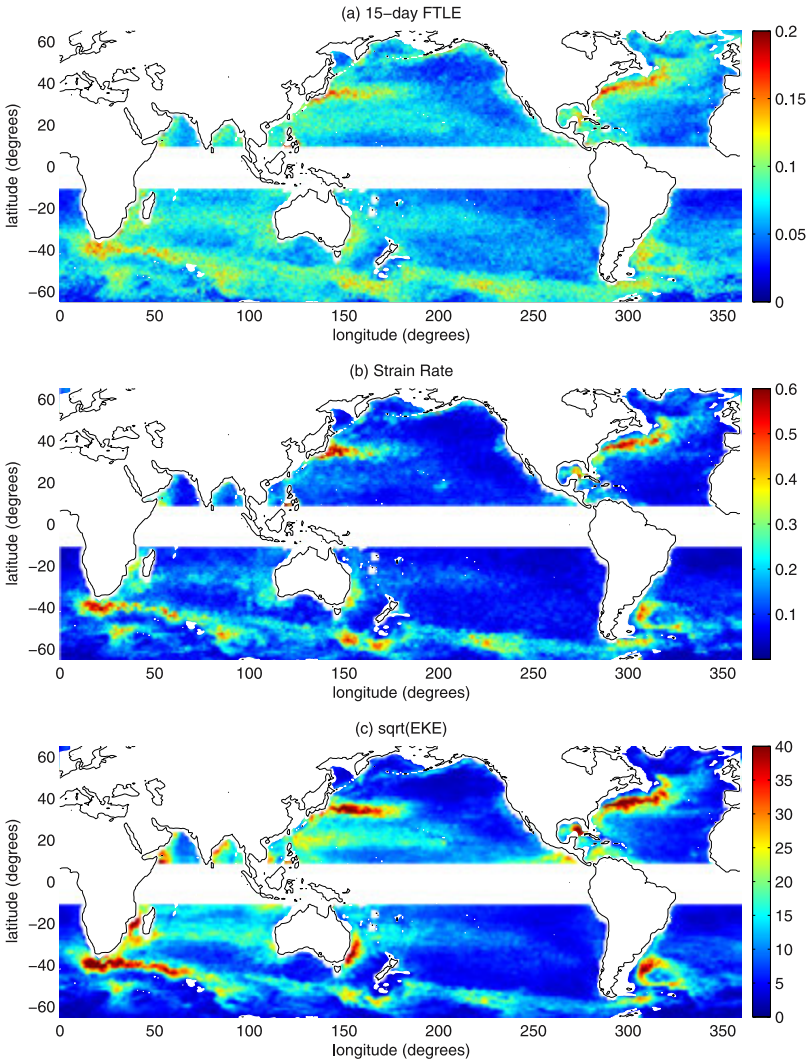

Figure 1. Maps of (a) ensemble mean 15-day FTLE <λ> (1/day), (b) time-mean strain rate <γ> (1/day), and (c) EKE$^{1/2}$ (cm/s). Areas shallower than 1000 m are not plotted.

within 10 degrees of the equator, and "global calculations" refer to calculations covering all the oceans outside 10 degrees of the equator. Thirty-day global calculations have been performed once per month (initialized at the start of each month) for 2002 and 2003. Additional longer calculations have been formed for limited regions and start dates.

[8] The variations in FTLEs are compared to those in the strain rate γ and the eddy kinetic energy EKE $= \frac{1}{2}<u'^2 + v'^2>$, where u' and v' are the deviations in the zonal and meridional velocities from the 2002–2003 mean values and the brackets denote a time average.

[9] Given the limited spatial and temporal resolution of the altimeter-based currents some caution is needed interpreting the FTLEs. However, as discussed by W06 there are several pieces of information that suggest the FTLE calculations may be reliable. Furthermore, more recent studies has shown good agreement between FTLEs and drifter trajectories [*Beron-Vera et al.*, 2008] and between finite size Lyapunov exponents and structures in satellite observations of chlorophyll and sea surface temperature [*Lehahn et al.*, 2007].

3. Results

3.1. Global Distribution

[10] The distribution of the ensemble-mean 15-day FTLE, <λ>, is shown in Figure 1a (<λ> is the mean λ at each location over the series of monthly calculations). This shows that the global distribution of the time-mean stirring is highly non-uniform, with high values in the western boundary currents (WBCs) of each ocean and the Antarctic Circumpolar Current (ACC), and low values in the eastern subtropics of each ocean. Also shown in Figure 1 are <γ> (Figure 1b) and EKE$^{1/2}$ (Figure 1c). As expected from W06, the variations in stirring is closely related to variations in mesoscale activity, with high or low values of the three quantities in the same regions. The distribution of FTLEs is also similar to calculations of lateral diffusivity from altimetry [e.g., *Stammer*, 1998] or dispersion of surface drifters [e.g., *Zhurbas and Oh*, 2004].

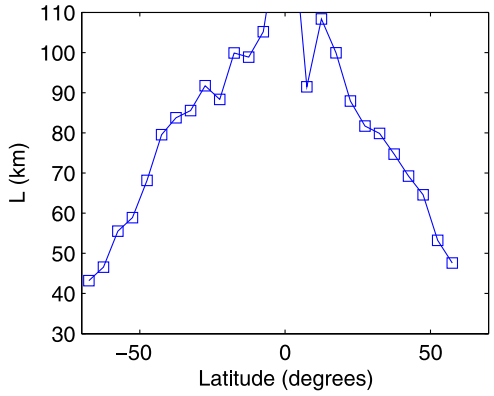

Figure 2. Latitudinal variation of the length scale L, derived from linear fits to $EKE^{1/2}$-$<\gamma>$ relationship. L is determined from a linear fit between $EKE^{1/2}$ and $<\gamma>$ for 5° by 5° regions within 10° latitude bands.

[11] W06 showed that $EKE^{1/2}$ $L <\gamma>$ (with L 80 km) in the Tasman Sea, and interpreted L as the eddy length scale. Such a linear relationship between $EKE^{1/2}$ and $<\gamma>$ is found in all oceans, although L decreases with latitude (see Figure 2). The latitudinal variation of L is similar to the Rossby radius of deformation of the first baroclinic mode L_R [*Chelton et al.*, 1998] and eddy length scale L_0 estimated from zero crossing of autocorrelation function of the altimeter data [*Stammer*, 1998], with $L_R < L < L_0$. As discussed by *Stammer* [1998], a correspondence between the eddy length scale and the Rossby radius supports the idea that the baroclinic instability is the primary source of the eddies.

[12] Given the above quantitative relationship between γ and EKE we focus now on the relationship between λ and γ. The details of this relationship depends on the integration time τ of the FTLE calculations. For short integration times λ γ, but λ decreases with increasing τ [e.g., *Abraham and Bowen*, 2000; W06]. This is illustrated in Figure 3a, which shows $\bar{\lambda}(\tau)$ for several 20° longitude by 20° latitude regions in the North Atlantic (here $\bar{\lambda}$ is the spatial mean λ over all points in each region from a single FTLE calculation). The spatial-mean strain rate, $\bar{\gamma}$, for each region is plotted at $\tau = 0$. For all regions $\bar{\lambda}$ decreases with time, with a more rapid decay for regions with larger $\bar{\gamma}$. The difference in FTLEs between regions with different $\bar{\gamma}$ decreases with integration time. This homogenization of the FTLE field is consistent with theoretical expectations [*Tang and Boozer*, 1996], however the convergence is very slow and there is still incomplete homogenization for calculations out to 300 days (not shown).

[13] The decrease of $\bar{\lambda}$ with τ, and dependence on mean strain rate, shown in Figure 3a occurs for other oceans and for different domain sizes. This is illustrated in Figure 3b which shows the variation of the 5-day, 10-day and 20-day $\bar{\lambda}$ with $\bar{\gamma}$, for 20° by 20° regions covering all oceans. The $\bar{\lambda}$-$\bar{\gamma}$ relationships are reasonably compact, i.e., small variation in $\bar{\lambda}$ for given $\bar{\gamma}$, and there appears to be a universal relationship across all oceans. For small strain rates $\bar{\lambda}$ $\bar{\gamma}$, but as the mean strain increases $\bar{\lambda}$ becomes less than $\bar{\gamma}$ (see W06). This, and other such plots, suggests that there is a universal relationship for $\bar{\lambda}(\tau)$ for regions with the same mean strain rate.

3.2. PDFs

[14] To further quantify the variations in the stirring we examine probability distribution functions of FTLEs, $P(\lambda)$. These distributions are calculated for λ from all grid points within a given domain, and PDFs have been calculated for domain sizes ranging from ocean basins down to 5° by 5° regions.

[15] For all regions the PDFs of λ have similar shape. The distributions are broad and asymmetric, with a peak at small stretching rates and a long high-stretch tail. The width and peak values of the PDFs varies with integration time τ, as illustrated in Figure 4a. For τ = 5 days $P(\lambda)$ is very similar to $P(\gamma)$, and as τ increases the $P(\lambda)$ distributions narrow and shift to lower values (see W06 and references therein). Although the mean and peak values decrease with τ the shape of the distributions remain similar. The self-similar structure of the PDFs can be seen by comparing the PDFs of λ normalized by the mean value $\bar{\lambda}$ (see Figure 4b).

[16] The characteristics of the PDFs also vary between regions, with broader distributions for regions with larger mean strain rates. There again appears to be a universal

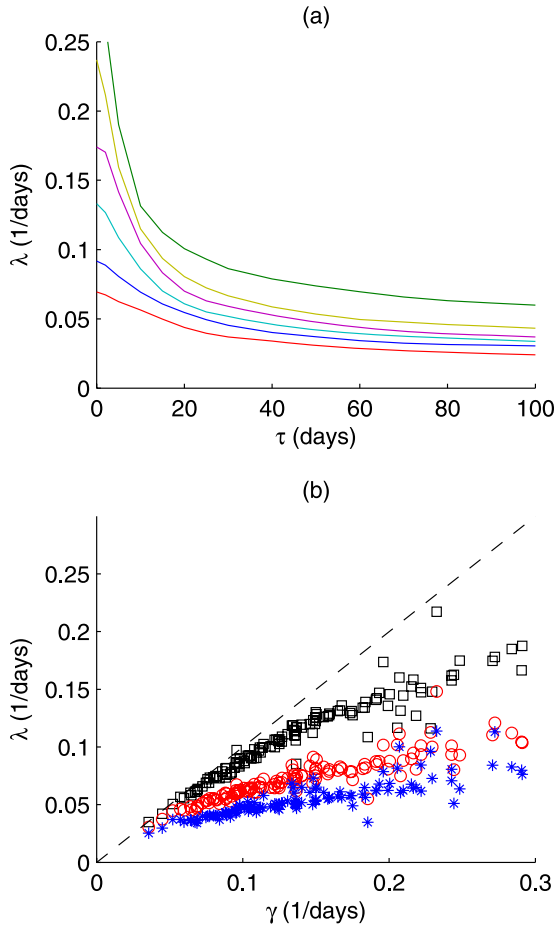

Figure 3. Variation of spatial-mean λ with (a) integration time τ, for several different 20° by 20° regions in the North Atlantic, and (b) spatial-mean strain rate $\bar{\gamma}$ for 20° by 20° regions in different oceans, for 5 (black), 10 (red) and 20 (blue) day integration times. Figures 3a and 3b show results for a single FTLE calculation initialized on January 1, 2002.

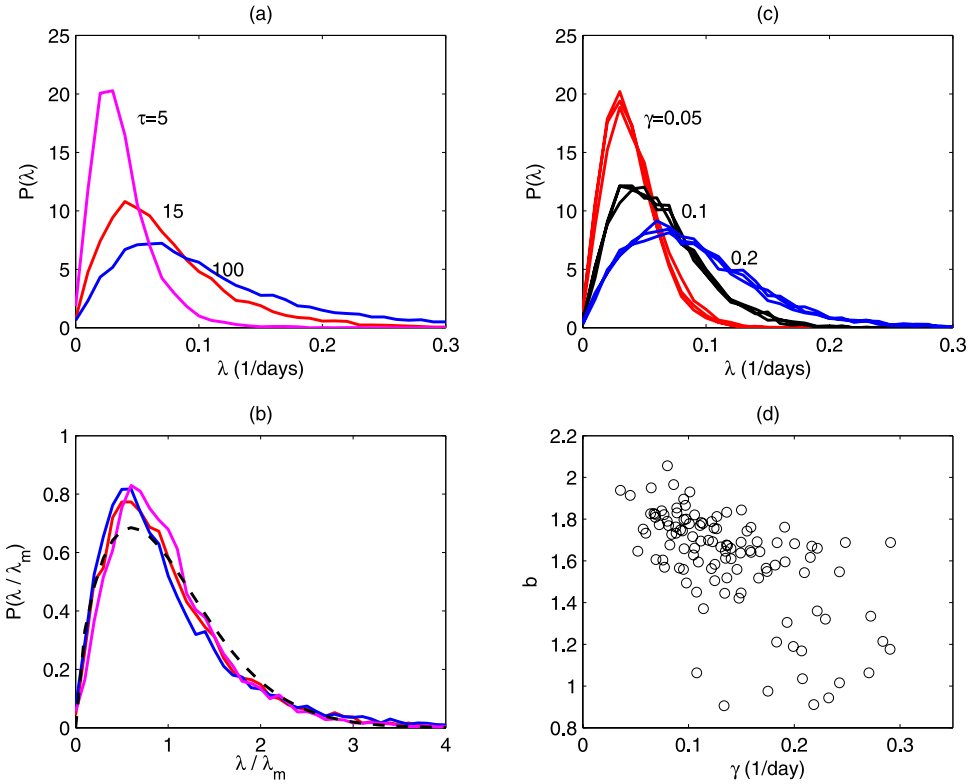

Figure 4. Variation of PDFs of λ with integration time τ and region. (a) PDFs for North Atlantic Ocean for several τ, for same calculation as shown in Figure 3a. (b) As in Figure 4a except for λ normalized by mean value. The dashed curve shows the Weibull distribution for b = 1.6. (c) PDFs of 15-day λ for several different 10° by 10° regions. The mean strain of the regions $\bar{\gamma}$ are 0.05 (red curves), 0.1 (black), and 0.2 (blue) 1/day. (d) Variation of the shape parameter b with $\bar{\gamma}$, for the Weibull distribution that best fits PDFs of 15-day λ for different 20° by 20° regions.

relationship across all oceans, with very similar P(λ) for regions with the same $\bar{\gamma}$. This is illustrated in Figure 4c which shows the PDFs of 15-day λ for multiple 10° by 10° regions that have similar values of $\bar{\gamma}$.

[17] W06 showed that the PDFs of λ in the Tasman Sea are reasonably well modeled by Weibull distributions

$$P(\lambda) = \frac{b}{a}\left(\frac{\lambda}{a}\right)^{b-1} \exp\left(\frac{\lambda^b}{a^b}\right), \qquad (2)$$

with $a = \bar{\lambda}/0.9$ and $b = 1.6$. This also applies for the Atlantic and other ocean regions. The dashed curve in Figure 4b shows a Weibull distribution with $b = 1.6$, which is a reasonable fit to the PDFs. There is a general tendency for the PDFs in weak strain regions to be better fit by $b = 2$ (Rayleigh distributions), whereas for large-strain regions the PDFs are more asymmetric and better fit by a Weibull distribution with $b = 1.4$ 1.6. Figure 4d shows the variation of the shape parameter b that best fits P(λ) with mean strain rate, for the different regions used in Figure 3b. The value of b also, generally, increases with τ and is around 2.5 to 3.0 for $\tau = 300$ days (not shown). In the very long-term limit the distributions might be expected to converge to a Gaussian distribution [*Tang and Boozer*, 1996], which corresponds to b around 3.6.

[18] The differences in b for regions with different strain implies differences in the distribution of the normal and shear components of strain (and hence velocity gradients). The PDF of the strain rates would be Rayleigh distributions if the distributions of the normal and shear components of the strain were Gaussian with zero mean and the same variance. The deviation of the strain rate PDFs from Rayleigh distributions suggests that the velocity gradients PDFs are non-Gaussian in these regions. The variations of b with mean strain rate is consistent with analysis of *Llewellyn Smith and Gille* [1998] and *Gille and Lleweyllen Smith* [2000], who showed that PDFs of velocity and velocity gradients are well fit by exponential distribution in western boundary currents and the ACC, but away from these regions the distributions are approximately Gaussian.

4. Conclusions

[19] Global calculations of FTLEs show that stirring in the surface ocean is highly non-uniform, and the characteristics vary with mesoscale activity. The PDFs of the FTLEs are broad, asymmetric, and have long high-stretch tails, and vary between regions with different mean strain rates. There are larger mean values and broader distributions in regions of high strain rates and EKE, e.g., western boundary currents and the ACC. Although the PDFs vary with region they have a near-universal relationships with the mean strain of a region, that holds in all oceans, and are reasonably well fit by Weibull distributions.

[20] The characteristics of the PDFs also vary with integration time. For short integration times the PDFs of FTLEs are very similar to those of the instantaneous strain rate, and are very broad. For increasing integration time the PDFs narrow and shift to lower values. The convergence of the FTLEs to a single value is very slow, and differences in mean values for regions with different strain rates persist to at least 300 days (and likely much longer).

[21] The above variations in the stirring have possible implications for understanding the distribution of biogeochemical tracers. FTLEs are closely related to the dispersal of localized patches of tracer [*Abraham et al.*, 2000; *Martin*, 2003] and to the spatial gradients of tracers [*Neufeld et al.*, 2000; *Abraham and Bowen*, 2002]. It may therefore be expected that the variations in stirring between regions with differing mesoscale activity will produce variations in the dispersal of tracer patches (e.g., growth of phytoplankton patches) and spatial heterogeneities of tracers (e.g., SSTs and ocean color).

[22] The above results also raise the possibility of developing a simple parameterization of the distribution of stretching rates based on the, easily-calculated, EKE. Given the EKE of a region the mean strain rate can be estimated using the linear relationship between mean strain rate and $EKE^{1/2}$. The mean λ could then be estimated from empirical fits to above λ (τ) curves for different mean strain rates. Finally, the distribution of λ could be estimated assuming a Weibull distribution. The implementation and value of such a parameterization will be explored in a future study.

[23] **Acknowledgments.** The surface currents used were obtained from the Archiving Validation and Interpretation of Satellite Data in Oceanography (http://www.aviso.oceanobs.com/). This work was supported by grants from the Royal Society of New Zealand ISAT fund and from USA National Science Foundation.

References

Abraham, E. R., and M. M. Bowen (2002), Chaotic stirring by a mesoscale surface-ocean flow, *Chaos*, *12*, 373–381.

Abraham, E. R., C. S. Law, P. W. Boyd, S. J. Lavender, M. T. Maldonado, and A. R. Bowie (2000), Importance of stirring in the development of an iron-fertilized phytoplankton bloom, *Nature*, *407*, 727–730.

Beron-Vera, F. J., M. J. Olascoaga, and G. J. Goni (2008), Oceanic mesoscale eddies as revealed by Lagrangian coherent structures, *Geophys. Res. Lett.*, *35*, L12603, doi:10.1029/2008GL033957.

Chelton, D. B., et al. (1998), Geographical variability of the first baroclinic Rossby radius of deformation, *J. Phys. Oceanogr.*, *28*, 433–460.

Chiswell, S. M., J. Wilkin, J. D. Booth, and B. Stanton (2003), Trans-Tasman Sea larval transport: Is Australia a source for new Zealand rock lobsters?, *Mar. Ecol. Prog. Ser.*, *247*, 173–182.

d'Ovidio, F., V. Fernández, E. Hernández-García, and C. López (2004), Mixing structures in the Mediterranean Sea from finite-size Lyapunov exponents, *Geophys. Res. Lett.*, *31*, L17203, doi:10.1029/2004GL020328.

Gille, S. T., and S. G. Lleweyllen Smith (2000), Velocity probability distributions from altimetry, *J. Phys. Oceangogr.*, *30*, 125–136.

LaCasce, J. H., and C. Ohlmann (2003), Relative dispersion at the surface of the Gulf of Mexico, *J. Mar. Res.*, *61*, 285–312.

Lacorata, G., E. Aurell, and A. Vulpiani (2001), Drifter dispersion in the Adriatic Sea: Lagrangian data and chaotic model, *Ann. Geophys.*, *19*, 121–129.

Lehahn, Y., F. d'Ovidio, M. Lévy, and E. Heifetz (2007), Stirring of the northeast Atlantic spring bloom: A Lagrangian analysis based on multi-satellite data, *J. Geophys. Res.*, *112*, C08005, doi:10.1029/2006JC003927.

Llewellyn Smith, S. G., and S. T. Gille (1998), Velocity probability density functions of large-scale turbulence in the upper ocean, *Phys. Rev. Lett.*, *81*, 5249–5252.

Mahadevan, A., and J. W. Campbell (2002), Biogeochemical patchiness at the sea surface, *Geophys. Res. Lett.*, *29*(19), 1926, doi:10.1029/2001GL014116.

Marshall, J., E. Shuckburgh, H. Jones, and C. Hill (2006), Estimates and implications of surface eddy diffusivity in the Southern Ocean derived from tracer transport, *J. Phys. Oceanogr.*, *36*, 1806–1821.

Martin, A. P. (2003), Phytoplankton patchiness: The role of lateral stirring and mixing, *Prog. Oceanogr.*, *57*, 125–174.

Neufeld, Z., C. Lopez, E. Hernandez-Garcia, and T. Tel (2000), Multifractal structure of chaotically advected chemical fields, *Phys. Rev. E*, *61*, 3857–3866.

Pierrehumbert, R. T., and H. Yang (1993), Global chaotic mixing on isentropic surfaces, *J. Atmos. Sci.*, *50*, 2462–2480.

Rio, M.-H., and F. Hernandez (2004), A mean dynamic topography computed over the world ocean from altimetry, in situ measurements, and a geoid model, *J. Geophys. Res.*, *109*, C12032, doi:10.1029/2003JC002226.

Rossi, V., C. López, J. Sudre, E. Hernández-García, and V. Garçon (2008), Comparative study of mixing and biological activity of the Benguela and Canary upwelling systems, *Geophys. Res. Lett.*, *35*, L11602, doi:10.1029/2008GL033610.

Stammer, D. (1998), On eddy characteristics, eddy transport, and mean flow properties, *J. Phys. Oceanogr.*, *28*, 727–739.

Tang, X. Z., and A. H. Boozer (1996), Finite time Lyapunov exponent and advection-diffusion equation, *Physica D*, *95*, 283–305.

Waugh, D. W., E. R. Abraham, and M. M. Bowen (2006), Spatial variations of stirring in the surface ocean: A case study of the Tasman Sea, *J. Phys. Oceanogr.*, *36*, 526–542.

Zhurbas, V., and I. S. Oh (2004), Drifter-derived maps of lateral diffusivity in the Pacific and Atlantic oceans in relation to surface circulation patterns, *J. Geophys. Res.*, *109*, C05015, doi:10.1029/2003JC002241.

E. R. Abraham, Dragonfly, 10 Milne Terrace, Island Bay, Wellington 6023, New Zealand.

D. W. Waugh, Department of Earth and Planetary Science, Johns Hopkins University, Baltimore, MD 21218, USA. (waugh@jhu.edu)